



OPEN ACCESS

EDITED BY

Georgia Pe-Piper,
Saint Mary's University, Canada

REVIEWED BY

Boris Alekseevich Natalin,
Istanbul Technical University, Türkiye
Qiang Xu,
Southwest Petroleum University, China

*CORRESPONDENCE

Zeqi Li,
✉ lzqlizard@126.com
Liu Shugen,
✉ lsg@cdut.edu.cn

RECEIVED 05 September 2024

ACCEPTED 10 December 2024

PUBLISHED 23 January 2025

CITATION

Guo R, Li Z, Wu J, Liu S, Sun W, Wang P,
Deng B, You L and Liu Z (2025) The
Neoproterozoic Ediacaran Kaijiang-Xuanhan
paleo-uplift in the Sichuan Basin, Western
China.
Front. Earth Sci. 12:1491529.
doi: 10.3389/feart.2024.1491529

COPYRIGHT

© 2025 Guo, Li, Wu, Liu, Sun, Wang, Deng,
You and Liu. This is an open-access article
distributed under the terms of the [Creative
Commons Attribution License \(CC BY\)](#). The
use, distribution or reproduction in other
forums is permitted, provided the original
author(s) and the copyright owner(s) are
credited and that the original publication in
this journal is cited, in accordance with
accepted academic practice. No use,
distribution or reproduction is permitted
which does not comply with these terms.

The Neoproterozoic Ediacaran Kaijiang-Xuanhan paleo-uplift in the Sichuan Basin, Western China

Ran Guo^{1,2}, Zeqi Li^{1*}, Jianxue Wu², Shugen Liu^{1*}, Wei Sun¹,
Peng Wang², Bin Deng¹, Liwei You¹ and Zhiyi Liu²

¹State Key Laboratory of Oil and Gas Reservoir Geology and Exploitation, Chengdu University of Technology, Chengdu, China, ²Sichuan Geophysical Company of CNPC Chuanqing Drilling Engineering Company Limited, Chengdu, China

The structural characteristics and formation evolution of the Sinian Kaijiang-Xuanhan paleo-uplift play a foundational role in the formation and evolution of the Sichuan Basin. To comprehensively understand the structural characteristics and formation evolution of the Sinian Kaijiang-Xuanhan paleo-uplift, this paper, based on geological, logging, seismic, and drilling, further confirms the existence of the Sinian Kaijiang-Xuanhan paleo-uplift and provides a detailed study of its characteristics. The entire Ediacaran tectonic sedimentary framework of the Sichuan Basin was controlled by this northeast-trending paleo-uplifted area. The Dengying Formation in the Kaijiang-Xuanhan region and the Mianyang-Anyue-Changning region both exhibit a thinning trend, but the genetic mechanisms are different. The thinning in the former is the result of sedimentary control during the early stages of paleo-uplift, with the lower parts of the first and second stages being absent; in the latter region, this is due to subsequent erosion. During the deposition periods of the Doushantuo and Dengying formations, the Sichuan Basin was predominantly in a weak compressional state, forming the Kaijiang-Xuanhan paleo-uplift, with the main structural orientation being northeastward. By the late Dengying Formation and early Cambrian, the region experienced a weak extensional state, resulting in the development of the Mianyang-Changning rift, with the main structural orientation being north-northwestward. The Kaijiang-Xuanhan paleo-uplift underwent four stages: the incubation period (before the deposition of the Doushantuo Formation), the peak development period (during the deposition of the Doushantuo Formation), the decline period (during the deposition of the Dengying Formation), and the extinction period (during the Lower Cambrian deposition). The further confirmation and in-depth study of the Sinian Kaijiang-Xuanhan paleo-uplift enhances the understanding of the Neoproterozoic craton of the Sichuan Basin and enriches the theory of the formation and evolution of the Sichuan Basin.

KEYWORDS

Neoproterozoic paleo-uplift, Kaijiang-Xuanhan, petroleum accumulation, Sichuan Basin, China

1 Introduction

Since 2005, the Maghreb Petroleum Research Group (MRPG) at the University of London has led a global initiative to study Precambrian ancient hydrocarbon-bearing systems. The “Global Infracambrian Hydrocarbon Systems Conference,”

held in London in 2006 and Jammu, India, in 2008, greatly advanced foundational research and exploration of Precambrian hydrocarbon systems in regions like North Africa, India, North America, Africa, and Australia (Craig et al., 2009; Bhat et al., 2012). Simultaneously, with increased exploration efforts and advancements in exploration and development technology in major domestic oil and gas basins, there has been growing interest in China in exploring Precambrian ancient hydrocarbon systems in recent years (Cozzi et al., 2012; Craig et al., 2013; Grotzinger and Al-Rawahi, 2014; Shang et al., 2020).

A paleo-uplift is an uplifted structure formed during a specific geological period, often continuing to develop similarly in subsequent periods, although some may eventually disappear or even transform into depressions (Slack, 1981; Kang, 1988; Doré and Jensen, 1996; Peters et al., 2003; Lottaroli et al., 2009; Fernandes and Roberts, 2020). Uplifts are large, positive structural units within basins and are crucial for understanding basins' formation, evolution, and tectonic deformation. They are also key areas for hydrocarbon accumulation and exploration (Korsch et al., 1991; Tang et al., 2013; Leonov et al., 2020). In many oil-rich cratonic basins around the world, a significant number of oil and gas fields have been discovered around paleo-uplift and their slopes, such as in the Siberian Basin in Russia, the Permian Basin in North America, and the Illizi and Sirte Basins in North Africa (Narbonne and Aitken, 1995; Saylor et al., 1995; Valdiya, 1995; Fraser et al., 2007; Yu et al., 2008; Sato et al., 2016; Shang et al., 2020).

In the past decade, significant progress has been made in hydrocarbon exploration around paleo-uplift and their slopes in China's three major marine basins, leading to the discovery of a series of large and medium-sized oil and gas fields as well as important hydrocarbon shows (Huang et al., 1996; Liu et al., 2011; Zhao and Cawood, 2012; Zhou et al., 2014; Liu et al., 2021). Notable examples include the new sub-salt formations in the Jingbian Gas Field of the central paleo-uplift in the Ordos Basin, the northern slope of the Tazhong uplift and the southern slope of the Tabei uplift in the Ordovician of the Tarim Basin (Liu et al., 2012; Liu et al., 2014; Liu et al., 2021; Li S et al., 2015; Wang et al., 2019; Wang et al., 2024). In recent years, significant breakthroughs in hydrocarbon exploration have been made in the Leshan-Longnüsi paleo-uplift area in the central Sichuan Basin, leading to the discovery of gas reservoirs in the Lower Cambrian Longwangmiao Formation in Moxi and the Sinian Dengying Formation in Gaoshiti. To date, the proven geological reserves have reached $1.15 \times 10^8 \text{ m}^3$.

The discovery of the Leshan-Longnüsi paleo-uplift in the Sichuan Basin has sparked significant interest among oil and gas explorers and researchers in identifying and studying paleo-uplift. Particularly in the eastern Sichuan Basin, an exploration area covering nearly 80,000 km² has seen limited drilling activity, with only two exploratory wells penetrating the primary hydrocarbon-bearing Dengying Formation. This has led to considerable debate regarding the existence of a paleo-uplift in this region. For instance, Gu et al. (2016), using seismic data from four framework lines combined with field outcrops, were the first to propose the existence of the Sinian Xuannan-Kaijiang paleo-uplift in eastern Sichuan, suggesting that its formation mechanism was controlled by basement uplift and providing preliminary insights into its

vertical evolution and spatial characteristics. In contrast, Li W. et al. (2015), mainly using field outcrop data from the Daba Mountains, proposed that extensional activities occurred along the northern edge of eastern Sichuan during the Sinian period, which may have led to the development of a rift trough extending into the basin. Overall, there are significant disputes regarding the tectonic-sedimentary differentiation and evolution characteristics of the Sinian period, primarily due to the following reasons: (1) The lack of three-dimensional seismic data in the past resulted in unclear structural characteristics of the deep Dengying Formation, and the complexity of high-steep structures further complicated the accurate interpretation of deep subsurface data; (2) Earlier studies were mostly based on field profiles from surrounding areas, and it is only in the past 5 years that wells drilling through the Dengying Formation in this region have been completed (e.g., Well WT-1 in 2018 and Well YT-1 in 2023), with drilling in the neighboring central Sichuan region gradually increasing over time. As a result, previous understandings lacked constraints from subsurface geological data. Therefore, this paper, based on the latest drilling, 2D, and 3D seismic data from the region, aims to reveal the characteristics, formation, and evolution of the Sinian Kaijiang-Xuannan paleo-uplift and to explore the influence of tectonic-sedimentary differentiation during the Sinian period on hydrocarbon accumulation in the Sichuan Basin.

2 Geological setting

The global Grenville orogeny resulted in the formation of the Rodinia supercontinent around 1,100 Ma during the Mesoproterozoic, after which it entered a prolonged period of stable evolution (Li and Zhong, 2009). Globally, the breakup of Rodinia supercontinent to the formation of Gondwana continent lasted about 400my. The breakup of supercontinents is driven by the "super mantle plume theory" (Rino et al., 2008; Maruyama et al., 2007; Li and Zhong, 2009; Santosh et al., 2009) is the mainstream. At 750-720 Ma, the super mantle plume formed an ocean between the Australian plate, the East Antarctica plate, the Lauren continent and the South China plate, and the plates separated from each other (Li and Li, 2007). The peak of the Pan-African orogeny occurred between 640-610 Ma, ultimately leading to the formation of the Pannotia supercontinent, with the Paleozoic Gondwana supercontinent as its core. For this reason, Pannotia is also called the Greater Gondwana supercontinent (Li W et al., 2015) or the Pan-African supercontinent (Meert and Torsvik, 2003). During this period, the South China block, the Indochina block, and the Cimmerian terrane were located along the northwestern margin of the Arabian-Australian plate within the Pannotia supercontinent (Zhong and Huang, 1997; Zhao and Cawood, 2012; Li S. et al., 2015). Until 540-530 Ma, the closure of the Mozambique ocean marked the final convergence of Gondwana continent (Collins and Pisarevsky, 2005; Boger and Miller, 2004; Jacobs and Thomas, 2004). The western and eastern margins of the Yangtze Block formed the north-south-oriented Kangdian Rift and the northeast-oriented Nanhua Rift Basin, respectively (Dong et al., 2011; Smith, 2012). Three-dimensional seismic data and deep seismic profiles from hydrocarbon exploration have also revealed northeast-trending

extensional faults and associated near-horizontal stratigraphic features in the pre-Sinian basement of the Sichuan Basin (Ma et al., 2007; Dong et al., 2011; Zhong et al., 2014; Chen et al., 2021). These findings suggest the presence of northeast-oriented rift basins within the pre-Sinian basement of the Yangtze Block, likely controlled by the rifting processes of the Rodinia and Pannotia supercontinents. Moreover, the preserved subduction-collision structures beneath the basin's basement further indicate that after the Neoproterozoic rift basins were filled and constructed, the basement of the Sichuan Basin became almost entirely solidified and stable (Figure 2B; Chen and Chen, 1987; Burchfiel et al., 1995; Liu et al., 2008; Gu et al., 2016).

The main sedimentary strata in the study area from the Late Cryogenian to the Early Cambrian include the Nanhua System's Nantuo Formation, Ediacaran Doushantuo Formation, and Dengying Formation, as well as the Cambrian Maidiping Formation and Qiongzhusi Formation, along with their corresponding strata (Figure 1B). The Nantuo Formation of the Nanhua System is primarily composed of variegated glacial till mudstone and glacial till siltstone in shades of grayish green, grayish yellow, and light gray. A series of dating data indicates that the top boundary age of the Nantuo Formation is approximately 635 Ma, which closely corresponds to the Marinoan snowball Earth event (Condon et al., 2005; Zhou et al., 2014). Due to the high terrain of the Neoproterozoic Upper Yangtze region, the Nantuo Formation is mainly distributed in the Micang-Daba Mountain area in Northeast Sichuan and the eastern Yunnan region in Southwest Sichuan, with a typical thickness of less than 100 m (Wang et al., 2012). The Doushantuo Formation is primarily composed of black shale, intercalated with multiple layers of gray dolomite or phosphorite. In areas such as the southwest margin of the Sichuan Basin, the sedimentary thickness generally ranges from tens of meters to 200 m. It is completely absent near the Hannan ancient land in the northeastern margin of the Sichuan Basin (Wang, 1996; Kumar et al., 2021).

The Dengying Formation is primarily composed of grayish-white dolomite and limestone deposits, with significant variations in sedimentary thickness. Within the carbonate platform sedimentary area, the maximum thickness can reach more than 1000 m (Meng et al., 2011), and in the slope-basin sedimentary area, with thickness ranging from tens of meters to hundreds of meters (Zhu et al., 2015; Chen and Feng, 2019). The Dengying Formation in the Sichuan Basin and its surrounding areas can be divided into four members. The first member is primarily composed of argillaceous dolomite and micritic dolomite. The second and fourth members are primarily composed of dolomite formed by microorganisms, commonly including stromatolites, dendrolites, oncolites, and laminites. The third member is mainly composed of sandstone and shale. According to isotope dating, carbon isotope stratigraphy, biostratigraphy, and other data, the depositional time of the Dengying Formation is roughly constrained between 551 Ma and 542 Ma (Li, 1999; Chen et al., 2015; Zhou et al., 2008; Condon et al., 2005). The Maidiping Formation is characterized by its richness in small shell fossils (Steiner et al., 2007), primarily composed of argillaceous limestone and dolomite, with numerous siliceous and phosphatic intercalations (Zhu et al., 2015; Li et al., 2012). The Maidiping Formation only retains strata in the intra platform depression, and this set of strata is basically missing in the platform area and high edge (Li et al., 2012;

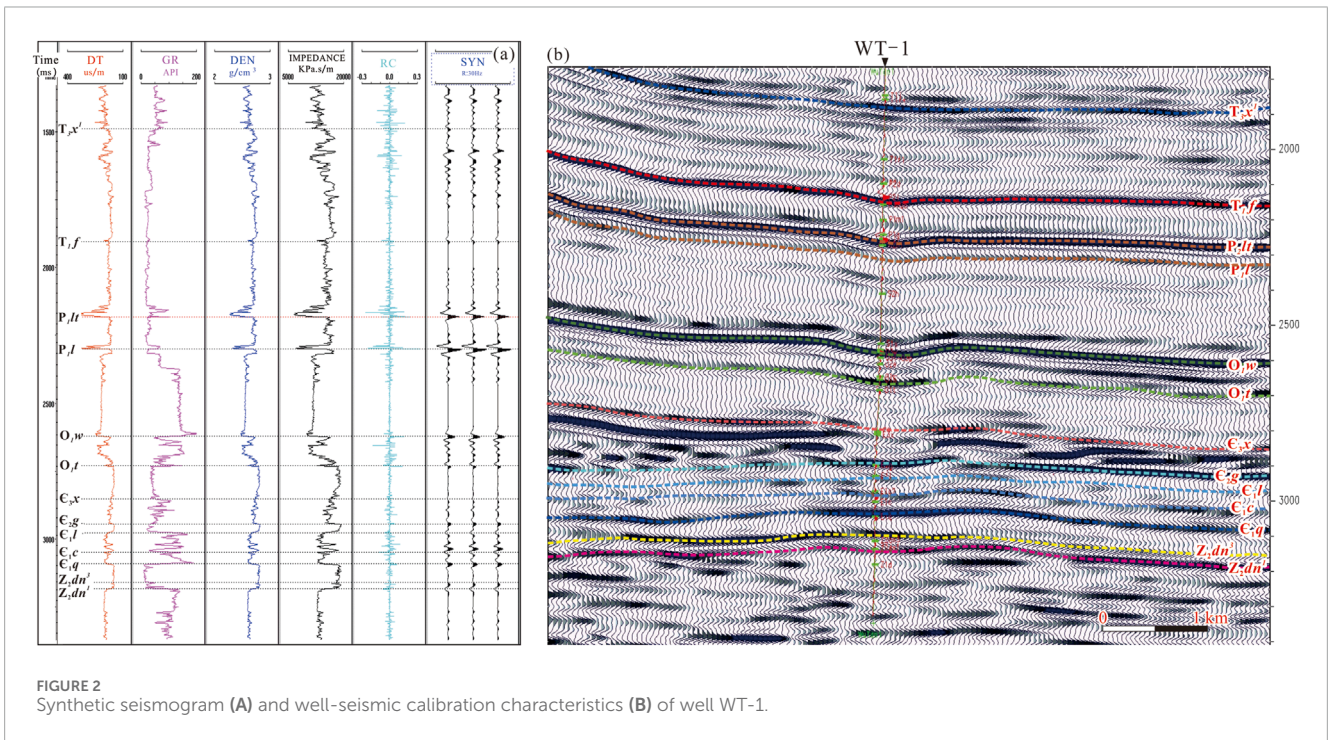
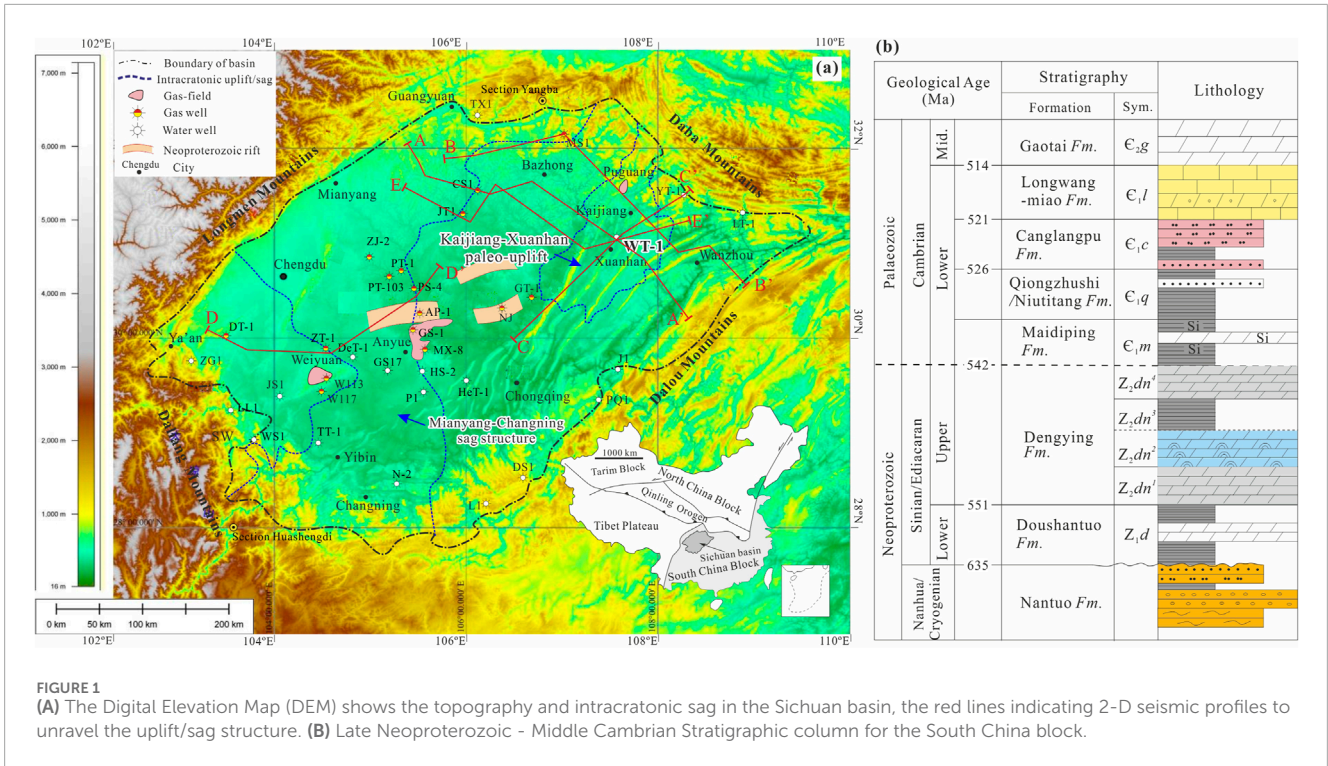
Okada et al., 2014; Zhu et al., 2015; Liu et al., 2021). The lithology of the Qiongzhusi Formation is primarily composed of black shale, often intercalated with siliceous rock, phosphorite, limestone interlayers, and limestone lenses. At the bottom, a polymetallic layer rich in Ni, Mo, and V is often developed, serving as a stratigraphic correlation marker (Lehmann et al., 2016; Han et al., 2017). The Re-Os dating results of the polymetallic layer and the underlying zircon ages indicate that the deposition of the Qiongzhusi Formation began approximately at 526–523 Ma (Chen et al., 2015; Wang et al., 2013).

3 Method and samples

3.1 Synthetic seismograms and precision interpretation of basin framework and 3D seismic data

The drilling of Well WT-1 reached the Cryogenian strata of the Neoproterozoic Nanhua System, with a final depth of 7,986 m, making the stratigraphic calibration particularly significant. Therefore, this paper primarily utilizes logging and seismic data from Well WT-1, supplemented by 13 other wells including YT-1, GS-1, NJ, PS-4, and W-117. Based on well-seismic calibration techniques that use standard horizon flattening and synthetic seismograms to enhance the accuracy of geological horizon interpretation (Ehsan and Abdolrahim, 2018), the major stratigraphic sequences in the seismic profiles are calibrated and interpreted (Figure 2). The specific methods are as follows: (1) Using CIFlog software to perform depth normalization of the logging data, the reflection coefficients are calculated from the acoustic and density logs, which are then convolved with the extracted seismic wavelet to obtain the initial synthetic seismograms; (2) Aligning the most prominent marker beds using a Ricker wavelet, followed by re-calibration with a statistical wavelet to adjust and align the major marker beds, and calibrating interlayer reflections with the deterministic wavelet; (3) Correcting the initial synthetic seismograms based on a more accurate velocity model, and matching them with seismic traces adjacent to the well to obtain the final synthetic seismograms.

Basin-scale seismic profiles are crucial foundational data for regional comprehensive studies. Besides geological information from drilling, logging, and outcrop studies, these profiles can provide a broader reflection of subsurface information, thereby reducing the ambiguity of research outcomes. To obtain high-quality seismic profiles and high-precision research results, this paper employs newly acquired basin-scale profiles combined with high-resolution 2D composite framework profiles. The principles for profile stitching are mainly as follows: (1) Selecting high-resolution survey grids as perpendicular as possible to ancient tectonic units; (2) Preferentially selecting grids passing through deep wells; (3) For 3D areas, extracting lines from 3D data for post-stack stitching, ultimately forming the basin-scale framework lines through superimposed stitching.



Based on the results of the synthetic seismic record calibration, well-seismic integration was used to select and evaluate 52 high-quality basin-scale framework profiles for basin-wide geological-seismic horizon interpretation and detailed stratigraphic tracking and correlation. The specific methods are as follows: (1) Using LANDMARK software to perform detailed well-seismic calibration on key deep wells along the 52 basin-scale framework profiles; (2)

Conducting detailed stratigraphic, fault, and structural correlation and interpretation of the major marker beds from deep to shallow in the framework profiles, establishing a geological-seismic stratigraphic framework for the major target horizons at the basin scale; (3) Using the framework profiles to correlate large-scale contiguous 3D seismic data, and conducting detailed correlation and interpretation of the 3D data.

3.2 Layer-flattened

The core principle of the horizon flattening method for paleo-geomorphological restoration posits that the distribution of depositional systems is governed by the dual influences of ancient geomorphological features and fluctuations in the base level. This method operates under the assumption that the depositional thickness of strata remains unaffected by compaction. Consequently, in this study, the depositional base level or the maximum flooding surface is employed as a reference baseline within the seismic data volume. The top and bottom surfaces of the targeted sequence are identified, and the temporal disparity between these surfaces is computed. The flattened top surface thereby represents the sea level at the time of original deposition, while the morphology of the bottom surface delineates the relative paleo-geomorphology preceding the deposition of the sequence. The methodological approach is as follows: (1) Conduct a comprehensive analysis of the basin's geological stratigraphy, structural characteristics, and fundamental features of paleo-uplift; (2) Leveraging the high-resolution seismic-geological integration and interpretation results previously discussed, carefully select the top and bottom reference surfaces for the principal sequence stratigraphy under investigation (e.g., the basal boundary of the Cambrian Gaotai Formation as corresponding to the top boundary of the Longwangmiao Formation, the basal boundary of the Cambrian corresponding to the top boundary of the Sinian Dengying Formation, the basal boundary of the third member of the Dengying Formation as aligning with the top boundary of the second member, and the basal boundary of the first member of the Dengying Formation as aligning with the top boundary of the Doushantuo Formation); (3) Utilize Landmark software to execute the horizon flattening process, with the resulting morphology of the bottom surface representing the relative paleo-geomorphology prior to the deposition of the sequence stratigraphy.

3.3 Thickness

The fundamental principle of the thickness method is based on the proportional relationship between the thickness of sedimentary layers and the age of the sediments. When sedimentary layers undergo erosion or denudation, the remaining sediments provide valuable insights into the ancient geomorphology. By measuring the thickness of these sediments, it is possible to infer the original thickness of the strata and the morphological characteristics of the paleo-geomorphology. The methodology is as follows: (1) Collect samples, including strata thickness revealed by drilling and geological outcrop profiles; (2) Perform physical and chemical analyses on the collected sediment samples; (3) Infer the morphological characteristics of the paleo-geomorphology by using Landmark software to subtract the corresponding seismic interpretation horizons, thereby calculating the time thickness of the strata. This time thickness is then converted into depth thickness values by fitting them to the stratigraphic thickness obtained from drilling. These values are then used to generate basin-scale maps in DoubleFox software, with local corrections made using thickness data from drilling and outcrops. When the thickness is substantial, it suggests a relatively thick original stratum, indicating

that the ancient geomorphology was likely a relatively elevated area; conversely, a smaller thickness may suggest a relatively lower area. (4) Based on multiple thickness maps, combined with geological and geomorphological principles, the evolutionary process of the ancient geomorphology can be inferred.

4 Result

4.1 Pre-cambrian onlap structures across the Sichuan Basin

In this paper, preferably selected are the two-dimensional and three-dimensional seismic data. Firstly, the formation calibration and interpretation of the profile are primarily utilizing the logging (Figure 2A) and seismic data from WT-1 well in combination with YT-1 well (Figure 2B). Based on the seismic synthetic record and seismic leveling technique, the main reflection interfaces of Precambrian overlying structures in the Sichuan Basin are as follows (Figure 3): (1) The cuttings from well WT-1 indicate that the lithology of the Nantuo Formation is primarily grayish-green sandy mudstone and argillaceous siltstone, and the seismic data are presented as random reflections or blank reflections; (2) According to the regional stratigraphic lithology, the Doushantuo Formation is mainly composed of mudstone and shale, and the bottom interface of the seismic data is characterized by strong wave crest reflections; (3) The base of the Dengying Formation (Z_2dn^1), the base of the third member of the Dengying Formation (Z_2dn^3), and the base of the Lower Cambrian Qiongzhusi Formation (ϵ_1q) are the boundaries between dolomite and mudstone, with distinctive reflection features. They represent relatively continuous strong reflection interfaces, generally exhibiting a single strong wave peak followed by a weak complex wave, with the single strong wave peak serving as the marker horizon. However, due to the influence of the piedmont tectonic zone, the interface at the anticline is not clear; the characteristics of the entire area are stable, with strong energy and good continuity, but the reflection at the structural axis is poor; (4) The Doushantuo Formation thins out towards the core of the paleoupift, with evident overlap (Figures 3B, C). Some reflection features are parallel. The high part of the paleoupift has a truncated relationship with the strong reflection interface at the base of the Dengying Formation, which is significantly different from the internal reflection characteristics of the Dengying Formation; (5) The reflection characteristics of the base of the Cambrian Longwangmiao Formation (ϵ_1l) are also influenced by lithological differences. A continuous medium-strong reflection interface is formed between the carbonate rocks of the Longwangmiao Formation and the underlying clastic rocks of the Canglangpu Formation, exhibiting a single strong trough with strong peaks before and after. The characteristics across the region are relatively stable with good continuity; (6) The mudstone at the bottom of the Upper Ordovician Wufeng Formation (O_1w) differs significantly from the limestone of the Middle Ordovician Baota Formation, forming a strong reflection interface. This shows a single strong wave peak followed by a wide complex wave with obvious waveform characteristics and good continuity, making it easy to identify, compare, and trace. The Piedmont structural zone can still be traced intermittently, which is a very important marker

bed interface in the study area and one of the important horizons for interpretation; (7) The carbonaceous mudstone at the bottom of the Upper Permian Longtan Formation (P_2lt) and the limestone of the Middle Permian Maokou Formation form a well-defined marker bed interface due to lithological differences, exhibiting a single strong wave peak, often accompanied by a strong phase above it. The study area features stable conditions and clear wave group characteristics, with good continuity and strong reflector energy, making it easily comparable and traceable. It can also be tracked in the piedmont structural zone, serving as an important traceable interpretation interface and one of the main standard reflectors in the study area; (8) The reflection interfaces between the Lower Triassic Feixianguan Formation (T_{1f}), the bottom of the Upper Triassic Xujiahe Formation (T_{3x}), and the Middle and Lower Jurassic are also clear. Due to extensive drilling, layer tracking and correlation are well-established (Liu et al., 2021). Through the tracking and comparison of the above horizons, combined with the control of some shallow exploration wells, the reliability of horizon interpretation in the study area is greatly improved, which can effectively support further interpretation and analysis.

Based on stratigraphic calibration and interpretation, the technique of horizon flattening was applied to the Cambrian basal interface to interpret the distribution and geometric characteristics of the Precambrian strata in the study area. The seismic profile within the Kaijiang-Xuanhan paleo-uplift exhibits the following features (Figure 3): (1) The seismic reflection axes show significant variation due to lithological changes, but when tracking across the entire basin, the thickness variation of the Doushantuo Formation is considerable. The thinning of the strata towards the Kaijiang-Xuanhan area is quite distinct, with the core of the paleo-uplift showing an overall absence or non-deposition of the Doushantuo Formation (Figure 3C). (2) Within the first and second members of the Dengying Formation, there is a clear onlap phenomenon towards the core area of the Kaijiang-Xuanhan paleo-uplift, indicating a transgressive feature during the deposition of the Dengying Formation (Figure 3D, E). (3) The deposition of the third and fourth members of the Dengying Formation is relatively stable, with minimal overall thickness variation. However, there is still a thinning trend towards the core area of the Kaijiang-Xuanhan paleo-uplift, where the third and fourth members of the Dengying Formation directly overlie the basement rock (Figures 3B, D, E).

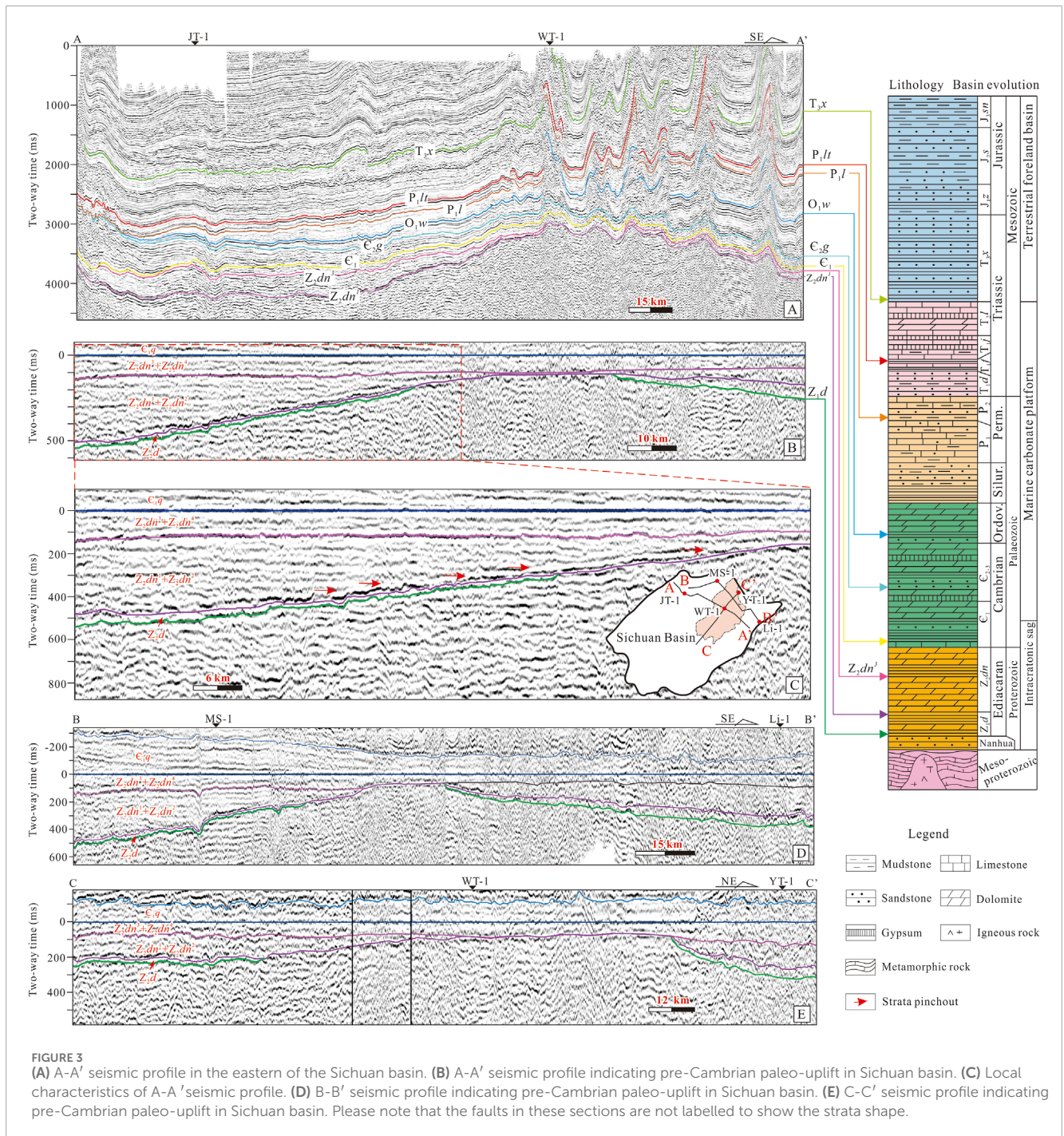
Through the above seismic profile features, combined with the thickness characteristics of the Doushantuo Formation along a northeast-to-southwest direction (Figure 4), it can be shown that in the early Late Sinian period, the Kaijiang-Xuanhan area had already formed a significant uplift, transitioning into broad, gentle slopes on both sides. The core of the paleo-uplift lacks the Doushantuo Formation and the first and second members of the Dengying Formation. On the flanks, the first and second members of the Dengying Formation onlap towards the core of the paleo-uplift, with the onlap more pronounced on the northwestern flank than on the southeastern flank. In the late Sinian period, the scale of the paleo-uplift's development weakened somewhat, with the third and fourth members of the Dengying Formation onlapping towards the core of the uplift. In the early Early Cambrian, there are still clear signs of onlapping deposition of the Qiongzhusi Formation on the northwestern side of the paleo-uplift, but the onlap is less evident on the southeastern side. By the mid-Early Cambrian, the scale of the

paleo-uplift's development gradually weakened, but weak onlapping deposition can still be observed, with the strata on the flanks of the paleo-uplift slightly thickening compared to the core, a trend that continued into the late Early Cambrian.

4.2 Characteristics of stratigraphic distribution in the Mianyang-Anyue-Changning area

From the geophysical profile, the thickness of the Dengying Formation in the Mianyang-Anyue-Changning area significantly thins, indicating a sudden change. The strong reflection at the base and the in-phase axes above it can be continuously traced and correlated, but the upper in-phase axes exhibit obvious truncation features, characteristic of erosional processes due to subsequent tectonic movements. In the Mianyang-Anyue area, the missing strata correspond to the upper part of the second member of the Dengying Formation. As shown in the profile in Figure 5, truncation features are widespread in the Mianyang-Anyue area, with the in-phase axes of the third member of the Dengying Formation exhibiting very pronounced truncation characteristics. These truncation features are more prominent in the northern part of the area and begin to weaken towards the south. It can be observed that the lower in-phase axes in the extensional trough area are continuous, with no signs of onlap or erosion, suggesting that during the deposition of at least the second member of the Dengying Formation, the extensional trough was a stable depositional environment without significant extensional features. However, in the adjacent Gaomo area, the strata are characterized by continuous parallel in-phase axes, with noticeable truncation towards the extensional trough. The third and fourth members of the Dengying Formation are missing in the Mianyang-Anyue-Changning area. The drilling results from Well PT-1, Well DeT-1, and Well PT-103 all indicate that the third and fourth members of the Dengying Formation are absent in the Mianyang-Changning extensional trough area (Figure 6).

The central Sichuan region is located on the eastern margin of the mid-section of the Mianyang-Changning Rift Trough (Liu et al., 2013). In this area, the Dengying Formation exhibits a trend of increasing stratigraphic thinning from the trough margin towards the interior of the trough. At the trough margin, wells GS-1 and MX-8 contain a relatively complete sequence of the four members of the Dengying Formation (Figure 6). In contrast, in the PT well area (e.g., wells PT-103 and PT-1) along the trough margin, the Dengying Formation shows significant thinning with the absence of the third and fourth members, and above the grape-like dolomite of the second member lies a phosphatic layer. This phosphatic layer contains small shell fossils, indicating its affiliation with the Cambrian Maidiping Formation (Liu et al., 2021). A few wells, such as PS-4, reveal that between the grape-like dolomite of the second member and the phosphatic layer of the Maidiping Formation, there is an intercalation of sandstone and mudstone, which may represent the third member, while the fourth member is absent. In Well DeT-1, located at the central part of the rift trough, the Dengying Formation exhibits well-developed grape-like structures, with the upper part of the second member missing and further thinning observed, indicating more significant erosion. In summary,



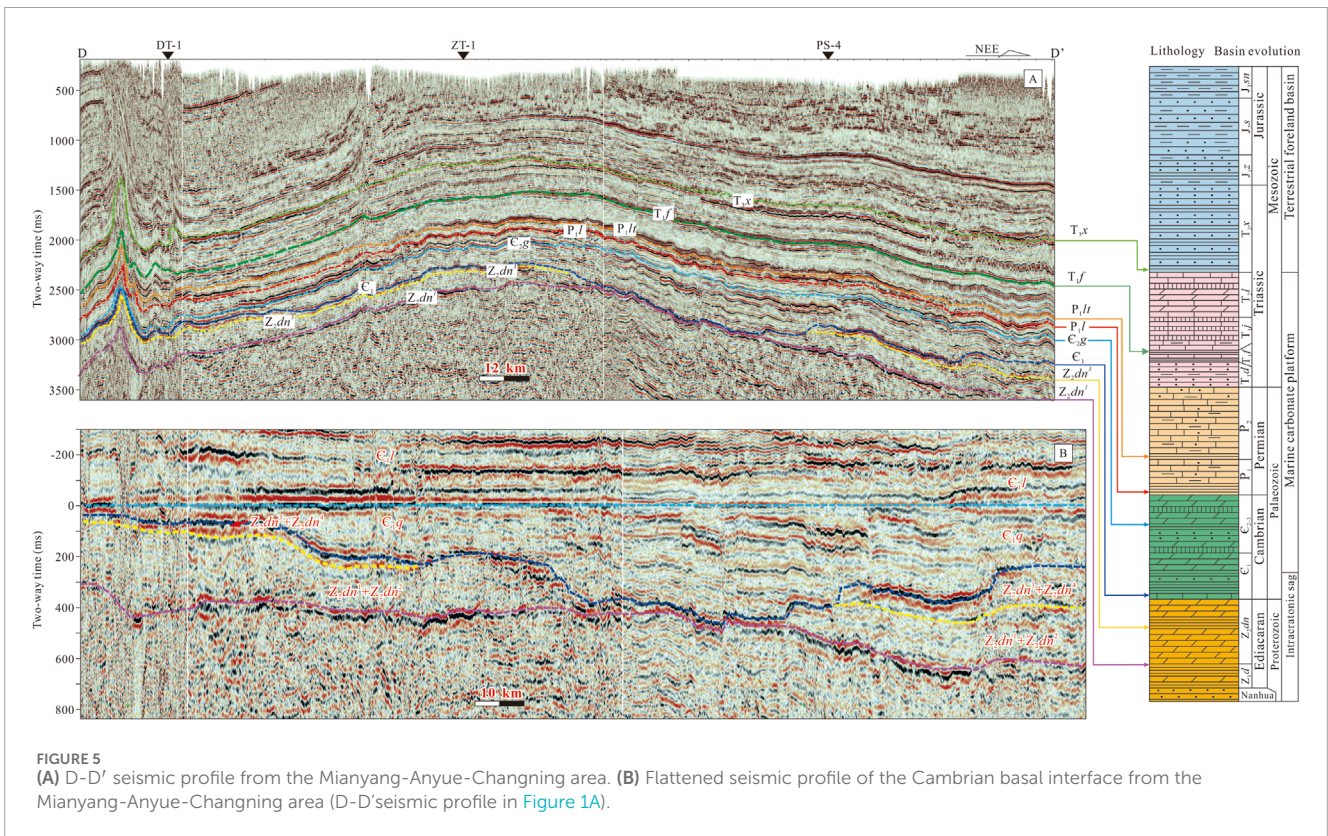
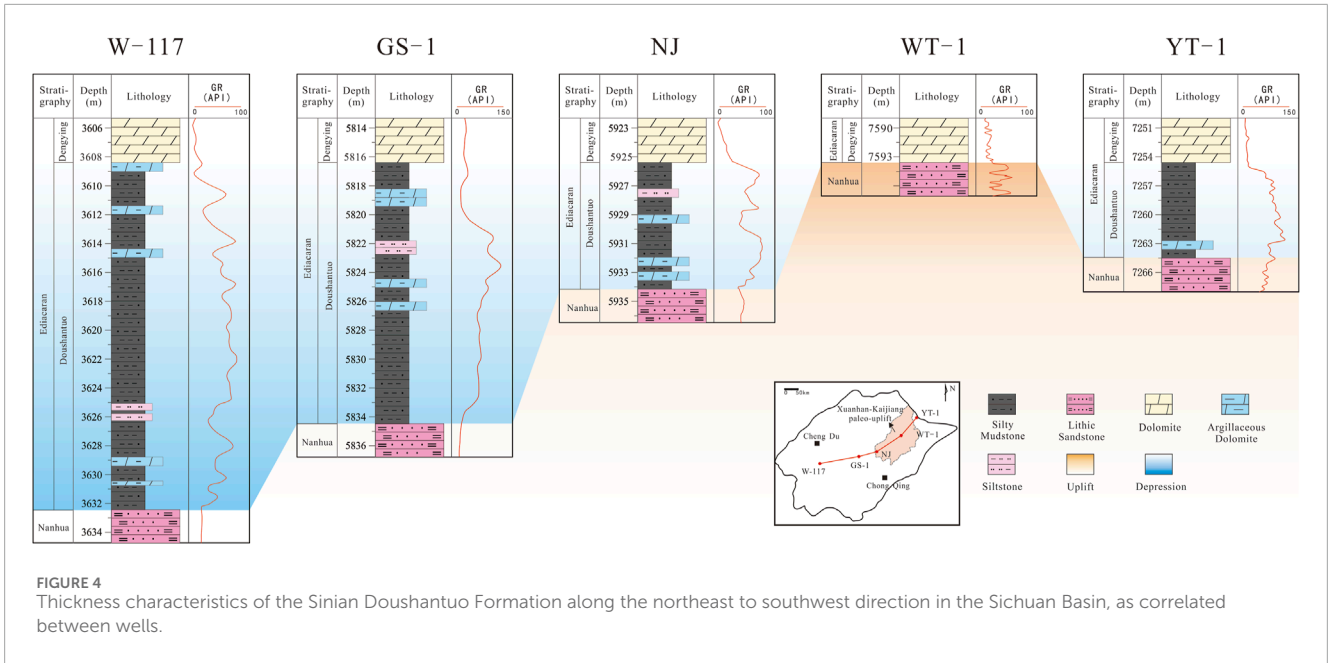
the thinning of the Dengying Formation in the Mianyang-Anyue-Changning area is due to the erosion of the third and fourth members and part of the upper strata of the second member. In contrast, in the Kaijiang-Xuanhan area (Well WT-1), the first member of the Dengying Formation is absent, while the third and fourth members are present (Figure 6). It is noteworthy that despite the significant thickness variations within and outside the rift trough, there is no substantial lithological change, particularly in the grape-like dolomite of the second member, which remains consistent inside and outside the trough. This consistency suggests a uniform depositional environment and indicates the absence of

significant tectonic activity that would have caused considerable lithological changes during this stage.

5 Discussion

5.1 Characteristics of the Neoproterozoic paleo-uplift in the Sichuan Basin

To reveal the distribution and evolutionary characteristics of the Kaijiang-Xuanhan paleo-uplift across the entire basin, this study,



in addition to utilizing the aforementioned basin-wide profiles, specifically employs data from 6 outcrop points on the basin's periphery and a total of 13 wells both within and around the basin. By selecting 52 seismic lines from 2D and 3D seismic data in the Sichuan Basin, covering a total of 20,182 km, and 32 blocks of 3D extracted lines, the study conducts detailed seismic stratigraphic

tracking and correlation, as well as seismic-geological integrated analysis. The focus is on the top and bottom of the Doushantuo Formation, the bottom and top of the third member and the top of the Dengying Formation in the Sinian system, as well as the Cambrian and Permian seismic reflection interfaces. Through these analyses, the study generates thickness maps for the Doushantuo

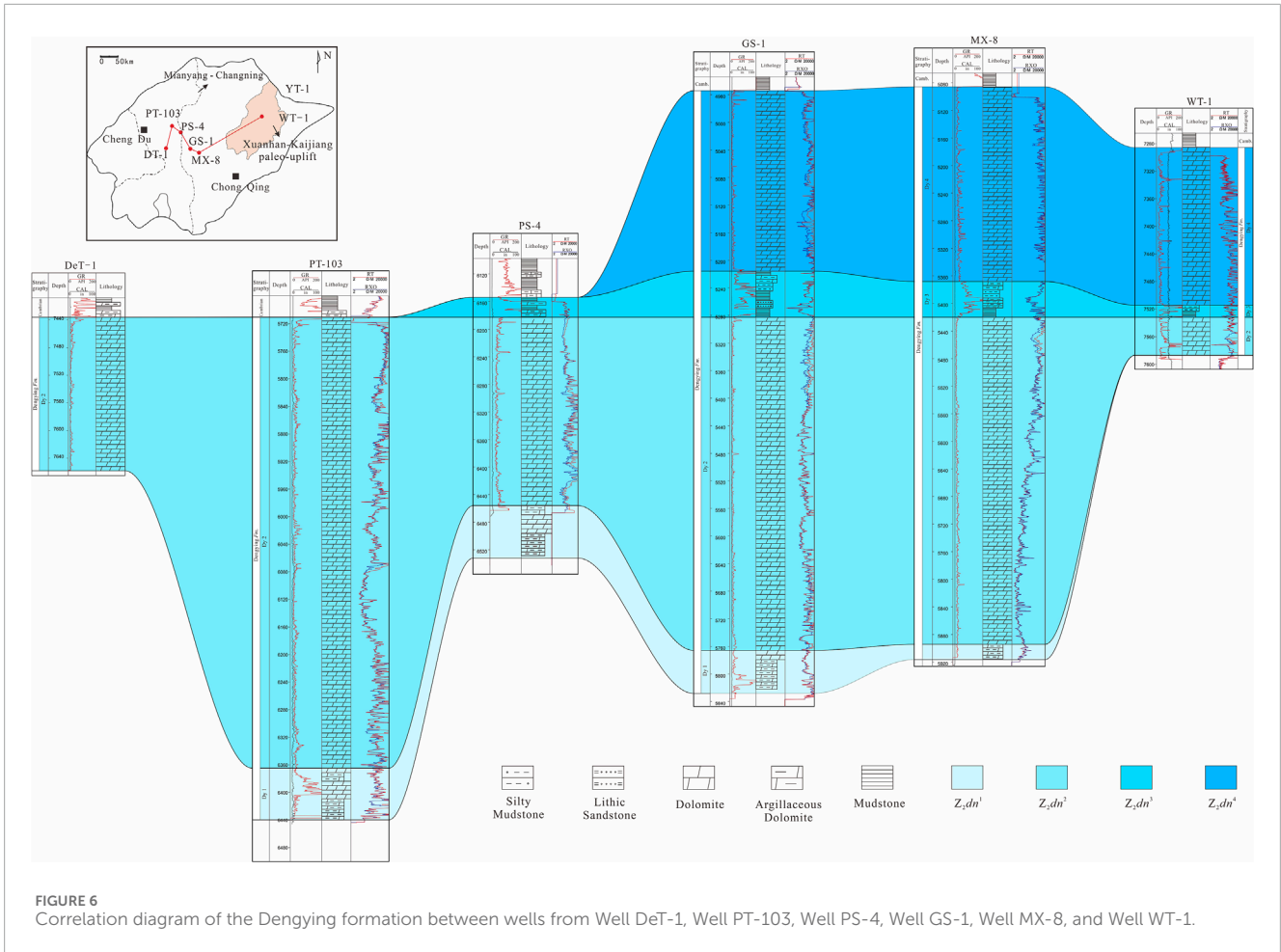


FIGURE 6 Correlation diagram of the Dengying formation between wells from Well DeT-1, Well PT-103, Well PS-4, Well GS-1, Well MX-8, and Well WT-1.

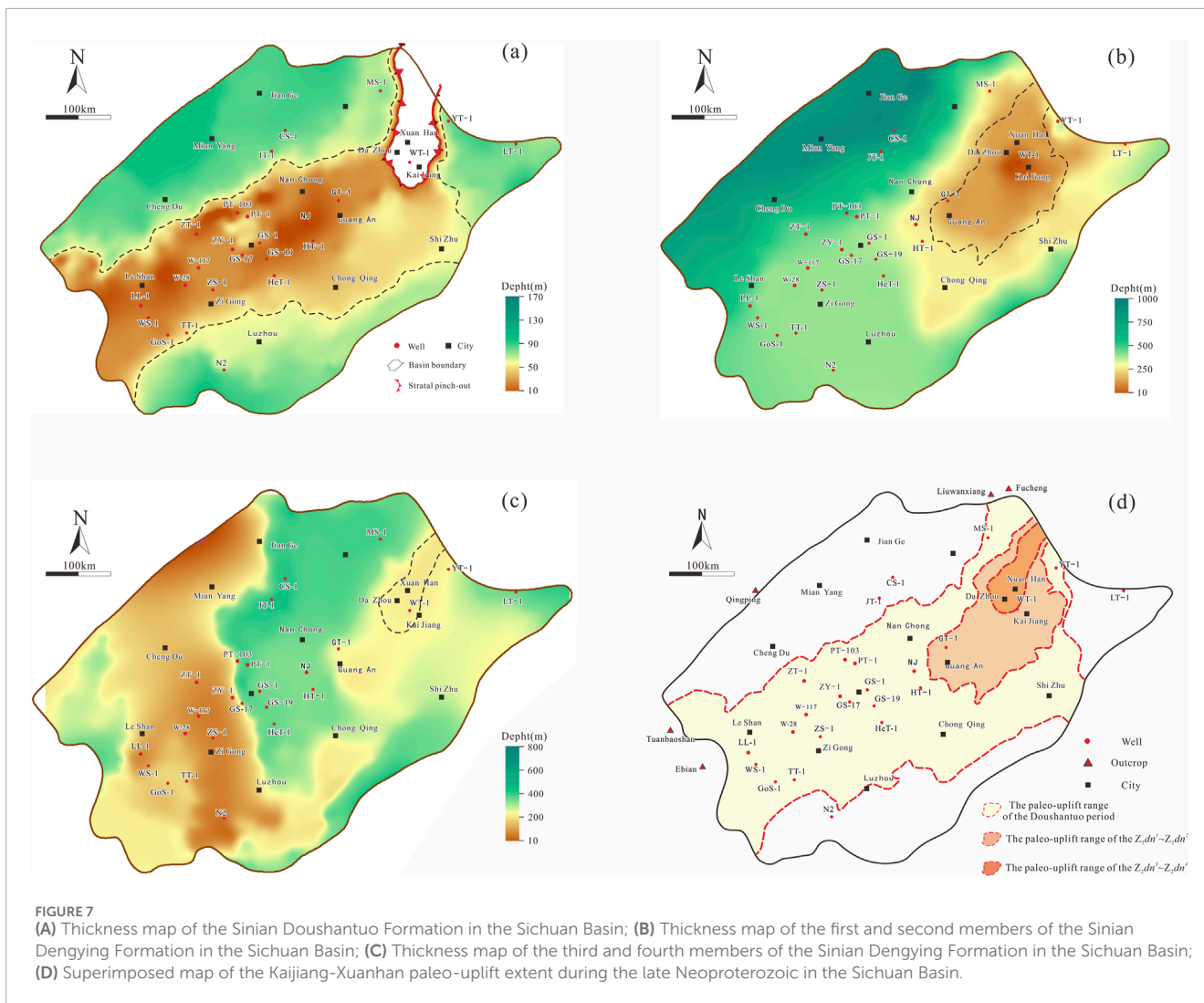
Formation, the Dengying Formation, and the Cambrian system, thereby revealing the characteristics of the Kaijiang-Xuanhan paleo-uplift (Figures 7, 8).

Using deep wells that penetrate the Doushantuo Formation within the basin, such as Wells Wei-117, Wei-28, Nüji, Laolong-1, PT-1, and PT-103, this study conducted precise calibration of the Doushantuo Formation’s basal interface. By fully utilizing the spatial continuity provided by the basin’s 3D seismic data and the seismic framework data, and by analyzing the thickness of the Doushantuo Formation encountered in wells both within and on the periphery of the basin, the study inferred the thickness variation trends of the Doushantuo Formation in areas without well control. This comprehensive approach allowed for the identification of the response characteristics of the Doushantuo Formation in different regions across the basin, thereby improving the reliability and accuracy of seismic tracking and correlation of the Doushantuo Formation’s basal interface.

Outcrops on the periphery of the basin reveal that the Doushantuo Formation has a significant thickness (200–550 m), with its lower part consisting of black shale and the upper part of carbonate rocks. In contrast, wells that penetrate or encounter the Doushantuo Formation within the basin show that its thickness is much smaller (0–53 m), although the lithological assemblage is similar to that observed in the outcrops. The Doushantuo Formation

is absent in the Shizhu-Kaijiang-Wanyuan area, indicating that this was the highest paleogeographic region before the deposition of the Dengying Formation (Figure 7A); the absence of the first member of the Dengying Formation suggests that this area was an emergent paleo-uplift during the early stages of Dengying deposition. The thickness of the Doushantuo Formation gradually increases from the Shizhu-Kaijiang-Wanyuan paleo-uplift towards both flanks. The thickness characteristics of the Doushantuo Formation, as revealed by well-seismic calibration and tracking, indicate that during the deposition of the Doushantuo Formation, the main structural feature within the basin was a “one uplift, three depressions” pattern. This consists of the Leshan-Anyue-Guangan-Kaijiang paleo-uplift (with its highest point in the Kaijiang area), and the western, southern, and eastern depressions, with slope zones in between. The thickness of the Doushantuo Formation increases progressively from the paleo-uplift towards both the eastern and western sides, but the two flanks are not completely symmetrical. The eastern flank of the paleo-uplift is gentle, with the Doushantuo Formation thickening towards the Changning area in the south and the western Hubei area in the north. The western flank of the Doushantuo Formation thickens rapidly towards the Chengdu-Deyang-Mianyang line.

During the deposition of the Doushantuo Formation, the paleo-uplift was well-developed, with its axis located along the



Leshan-Anyue-Guangan-Kaijiang line, primarily trending in a northeast-southwest direction. In the Kaijiang area, the Doushantuo Formation is absent, while in the Weiyan-Anyue region, its thickness ranges from approximately 10–65 m (Figure 7A). The paleo-uplift during the Doushantuo period covered a relatively large area, with its main body trending northeast (approximately 50°) to north-northeast (approximately 10°). The uplift extends from Dazhu in the northeast, turning to a north-northeast orientation, stretching from Leshan in the west to the Daba Mountains in the east, forming a spindle-shaped or obliquely elongated rectangle. The core area of the uplift is located around Dazhou-Xuanhan, where the Doushantuo Formation is absent. Moving westward towards the Guangan-Suining-Anyue-Leshan-Mabian line, the Doushantuo Formation remains relatively thin, marking the core of the paleo-uplift. The long axis of the core extends approximately 560 km, with a short axis of about 150 km, covering a total area of about 80,000 km². This indicates that during the deposition of the Doushantuo Formation, the Kaijiang-Xuanhan region represented the highest part of this paleo-uplift within the basin.

During the deposition period of the first and second sections of the Dengying Formation, the ancient uplift extended along the

Guangan-Xuanhan line, with its highest point located near Kaijiang. However, the scale of this uplift was significantly smaller compared to the ancient uplift during the deposition of the Doushantuo Formation. The long axis of the uplift was approximately 230 km, and the short axis was about 160 km, covering a total area of approximately 3.6×10^4 km². The orientation of the uplift remained consistent with that during the Doushantuo Formation deposition, trending northeast. The thickness of the first and second sections of the Dengying Formation ranged from approximately 30–300 m, with the thinnest section observed near Well WT- 1, where the first section is absent and the thickness of the second section is 59.7 m (Figure 7B). During this period, the Sichuan Basin exhibited a structural-depositional pattern of “one uplift and two depressions.”

The thickness distribution characteristics of the third and fourth sections of the Dengying Formation show significant changes compared to the first and second sections. The ancient uplift further contracted to the Kaijiang-Xuanhan area (Figure 7C), forming a structural-depositional pattern of “one uplift and two depressions,” specifically the Kaijiang-Xuanhan ancient uplift and the western and southern depressions, with the remaining areas being slopes.

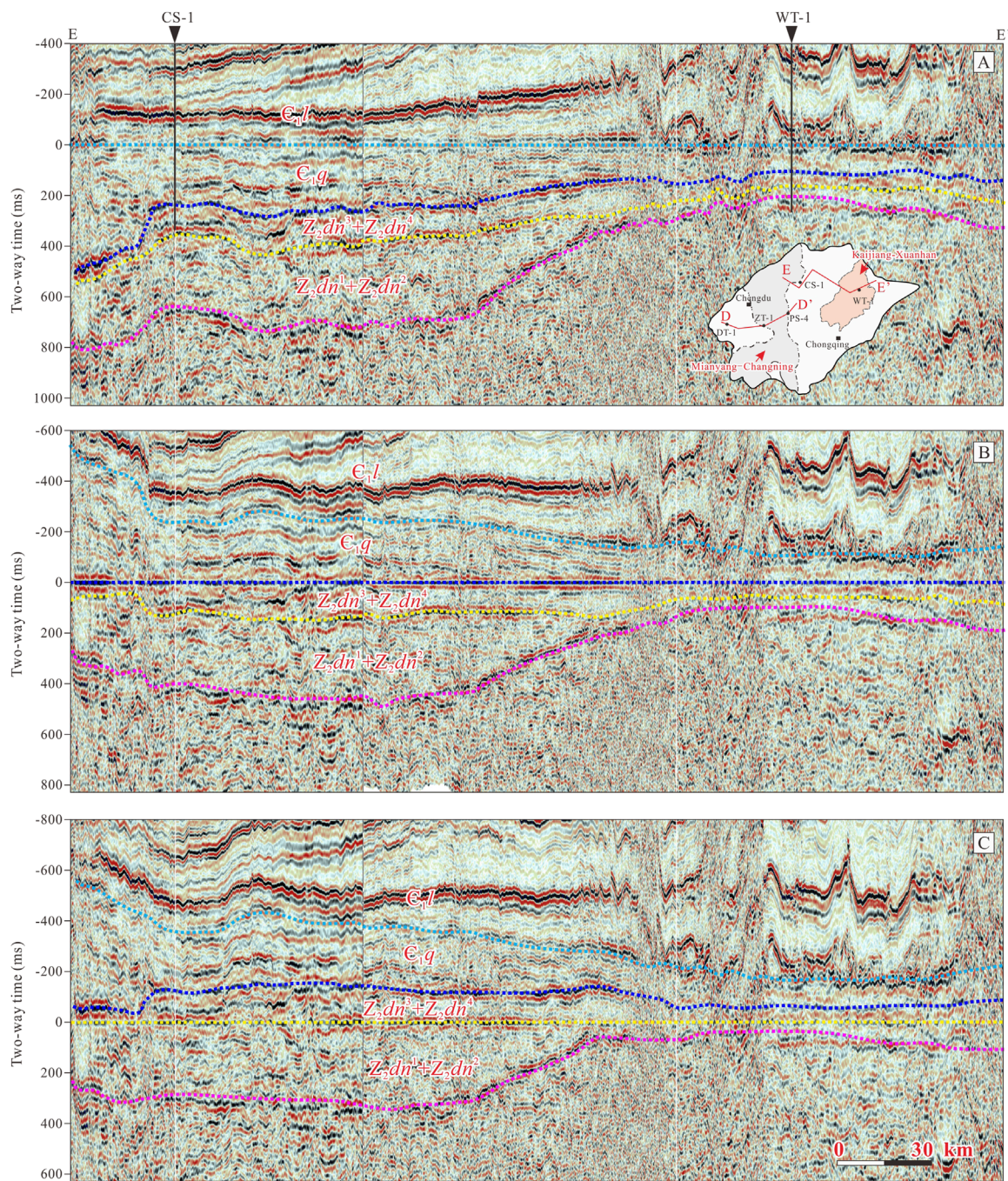


FIGURE 8 (A) E-E' seismic profile indicating the characteristic of Mianyang-Anyue-Changning area and the Kaijiang-Xuanhan area before Cambrian Longwangmiao Formation (ϵ_1/l) sedimentation. (B) E-E' seismic profile indicating the characteristic of Mianyang-Anyue-Changning area and the Kaijiang-Xuanhan area before Cambrian sedimentation. (C) E-E' seismic profile indicating the characteristic of Mianyang-Anyue-Changning area and the Kaijiang-Xuanhan area before The third member of sinian Dengying formation sedimentation.

During this period, the ancient uplift had significantly reduced in size compared to the deposition period of the second section, with a long axis of approximately 200 km and a short axis of about 80 km, covering a total area of approximately $1.4 \times 10^4 \text{ km}^2$. The core of the uplift contracted to the Chongqing-Xuanhan line, with the orientation still trending northeast, but its extent had

considerably diminished (Figure 7D). The thickness of the third and fourth sections of the Dengying Formation near Well WT-1 was 238.04 m, while the thickness across the entire uplift area was approximately 200–250 m. During this period, the Sichuan Basin continued to exhibit a structural-depositional pattern of “one uplift and two depressions.”

5.2 Differences between Kaijiang-Xuanhan region and Mianyang-Anyue-Changning region

To more clearly analyze and understand the characteristics of the paleo-uplift during the Dengying period (Kaijiang-Xuanhan paleo-uplift) and the rift trough region (Mianyang-Anyue-Changning area), the large framework cross-section of the Sichuan Basin, which transects the rift trough, was utilized. By flattening the bottom of the third member of the Dengying Formation and the base of the Lower Cambrian, the variations within the Dengying Formation across the Sichuan Basin can be more clearly demonstrated, revealing the characteristics and processes of the tectonic-sedimentary differentiation (Figure 8). Through comprehensive well-seismic analysis, the Dengying Formation in the Sichuan Basin is found to exhibit the following key characteristics:

- (1) The thickness distribution of the Dengying Formation, particularly the thickness of the first and second members, shows a wedge-shaped variation centered around the Kaijiang-Xuanhan ancient uplift in the northeast. The sedimentary thickness near the Kaijiang-Xuanhan ancient uplift is significantly reduced, with the Doushantuo Formation and the lower and middle parts of the first and second sections of the Dengying Formation being absent in the uplift area. The sedimentary thickness within the Mianyang-Changning rift trough differs considerably from that at the trough margin and the Kaijiang-Xuanhan ancient uplift area. Within the trough and at the trough margin, the third and fourth sections, as well as parts of the upper second section of the Dengying Formation, are absent.
- (2) The lithological variation of the Dengying Formation in the Kaijiang-Xuanhan ancient uplift area is a gradual process without a significant abrupt change. The thickness of the Dengying Formation is relatively stable in the western part of the Kaijiang-Xuanhan ancient uplift. From Well WT-1 to Well YT-1 and further north towards the Chengkou area, the thickness of the Doushantuo Formation shale is relatively large and stable, with minor occurrences of dolomite and siliceous dolomite, indicating a lower slope depositional environment. In contrast, drilling within and at the margin of the Mianyang-Changning rift trough reveals no evidence of slope depositional deformation (slump blocks or soft-sediment deformation), and the lithology in both the rift trough and its margin is uniformly dolomite.
- (3) Seismic profiles in the Kaijiang-Xuanhan paleo-uplift area show an obvious onlapping of the first and second sections of the Dengying Formation onto the ancient uplift. In the Mianyang-Changning rift trough, the continuous reflectors in the lower part of the Dengying Formation indicate continuous strata, while the middle and upper reflectors exhibit significant truncation features, likely due to later tectonic movements and erosion.

In summary, while both the Kaijiang-Xuanhan area and the Mianyang-Anyue-Changning area exhibit thinning of the Dengying Formation, the causes of this thinning are likely different (Table 1). The thinning in the former is due to early non-deposition controlled

by the ancient uplift, whereas in the latter, it is due to late-stage erosion after the deposition of the Dengying Formation.

5.3 Evolution of the Kaijiang-Xuanhan paleo-uplift

5.3.1 The peak development period of the Kaijiang-Xuanhan paleo-uplift

The Kaijiang-Xuanhan ancient uplift may have been in its incubation phase prior to the deposition of the Doushantuo Formation, with the basement of the Sichuan Basin possibly already displaying characteristics of an ancient uplift (Gu et al., 2016). After the Nantuo glaciation, sea levels rose, and the Doushantuo Formation was extensively deposited across the craton. However, in the high areas of the ancient uplift, such as the Kaijiang-Xuanhan region, no deposition occurred, while relatively thick deposits of the Doushantuo Formation, reaching thicknesses of 200–300 m, accumulated in the slope and depression zones (Figure 7A). The period during which the Doushantuo Formation was deposited in the Kaijiang-Xuanhan area is likely the time when the ancient uplift within the Sichuan craton was most developed, as evidenced by its large scale and pronounced uplift characteristics. For instance, Well WT-1 shows an absence of the Doushantuo Formation, whereas the thickness of the Doushantuo Formation increases significantly on both the eastern and western sides of Well WT-1. During this period, the structural-depositional pattern of the Sichuan Basin was characterized by one uplift and three depressions, with the highest region of the uplift located along the Kaijiang-Xuanhan line, trending northeast. The Doushantuo Formation on both sides of the ancient uplift unconformably overlapped onto the uplift (Figures 7A, 9A).

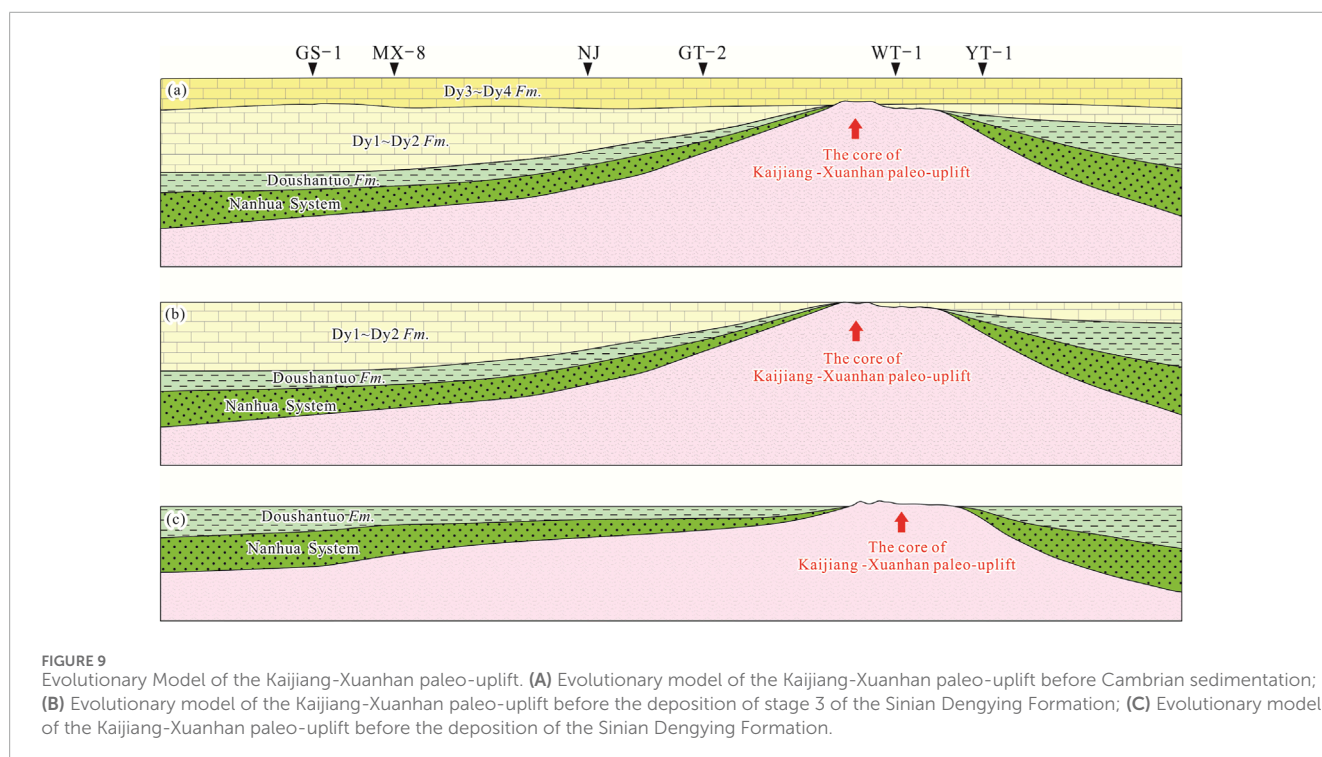
5.3.2 The recession period of the Kaijiang-Xuanhan paleo-uplift

During the early deposition of the Dengying Formation (stages 1 and 2; Figures 7A, B; Figures 9B, C), influenced by the continuous activity of the paleo-uplift, the core of the paleo-uplift remained exposed at the surface, resulting in the absence of Dengying stages 1 and 2 deposits in the core area of the Kaijiang-Xuanhan paleo-uplift. Towards the flanks, sediments from stages 1 and 2 of the Dengying Formation were deposited in the slope to sag regions (Figure 7B). Drilling results from Well WT-1 reveal a thickness of 60 m for stage 2 of the Dengying Formation, with only the topmost deposits of micritic dolomite and sandy dolomite preserved. Across the entire Sichuan Basin, the paleo-uplift had shrunk, retreating from the central basin to the central-eastern Sichuan area. However, the Kaijiang-Xuanhan region remained the elevated part of the paleo-uplift, with dolomite being the predominant sedimentary rock across the basin. By the end of stage 2 deposition of the Dengying Formation, the entire Sichuan Basin had been submerged, forming a submarine uplift (Figures 7B, 9B). Before the deposition of stage 3 of the Dengying Formation, the paleo-uplift in the Kaijiang-Xuanhan area continued to exhibit characteristics of an erosional-sedimentary paleo-uplift, with stages 1 and the lower part of stage 2 missing in its core region (Table 2).

During the late deposition of the Dengying Formation (stages 3 and 4), the core region of the Kaijiang-Xuanhan paleo-uplift

TABLE 1 Comparative characteristics of the Dengying Formation between the Kaijiang-Xuanhan paleo-uplift and the Mianyang-Changning extensional trough.

	Kaijiang-Xuanhan paleo-uplift	Mianyang-Changning extensional trough
Distribution range	Xuanhan-Dazhu-Wusheng-Ziyang line	Guangyuan-Mianyang-Changning line
Area	Approximately 60,000 km ²	Approximately 25,000 km ²
Developmental time	Incubation period: Before the deposition of the Doushantuo Formation Peak period: From the Doushantuo Formation to the Dengying Formation deposition period Decline period: Early Cambrian	Incubation period: Late stage of Dengying Formation deposition Peak period: From the Maidiping Formation to the Qiongzhusi Formation deposition period Decline period: During the Longwangmiao Formation deposition period
Strike	Northeast to North-Northeast (axis approximately 40°)	North-Northwest to nearly North-South
Stratigraphic characteristics	The core of the ancient uplift lacks the Doushantuo Formation, the first section, and the lower part of the second section of the Dengying Formation. (Non-depositional absence)	The rift trough lacks the fourth section, the third section, and the upper part of the second section of the Dengying Formation. (Later-stage erosion)



transitioned into a submarine uplift. The extent of absence or thinning in the upper Dengying Formation (stages 3 and 4) was less pronounced compared to the lower Dengying Formation (stages 1 and 2). At this stage, the paleo-uplift within the basin had significantly contracted, remaining primarily in the eastern Sichuan region around Kaijiang-Xuanhan, while the entire basin was submerged under seawater, resulting in the deposition of carbonate strata (Figures 7C, 9C; Table 2). During this period, erosional (or denudational) processes intensified in the Mianyang-Anxian-

Changning area, leading to the erosion of the upper part of stage 2, as well as stages 3 and 4 of the Dengying Formation. The tectono-sedimentary pattern of the Sichuan Basin underwent significant changes by the end of the Dengying Formation deposition. The basin shifted from a weakly compressional regime, characterized by the development of the northeast-oriented paleo-uplift (Kaijiang-Xuanhan paleo-uplift), to a weakly extensional regime, marked by the development of the northwest-oriented Mianyang-Changning extensional trough (Liu et al., 2013).

TABLE 2 Evolution and tectono-sedimentary differentiation characteristics of the Sinian Kaijiang-Xuanhan paleo-uplift.

	Peak stage: During the deposition of the Doushantuo Formation	Decline stage: during the deposition of the Dengying Formation	Extinction stage: During the deposition of the lower Cambrian
Sedimentary characteristics	The core region lacks the Doushantuo Formation, while the slope and sag areas have relatively thick deposits of the Doushantuo Formation	Inheriting the paleotopography of the Doushantuo Formation, the elevated part of the paleo-uplift lacks the lower and middle sections of Dengying Formation Member 1 and Member 2	The paleo-uplift topography disappeared, and the development of the Mianyang-Changning extensional trough led to the formation of a platform-trough topography
Lithofacies assemblage	Interbedded light gray thin-bedded medium-grained quartz sandstone, light gray thin- to medium-bedded gravelly coarse sandstone, light to medium gray thin-bedded micritic dolostone, and medium gray thin-bedded medium- to coarse-grained sandstone	The first, second, and fourth members of the Dengying Formation are composed of dolostone, while the third member consists of clastic rocks. The second and fourth members of the Dengying Formation are mainly dolomites formed by various microorganisms, such as thrombolites, dendrolites, Oncolites etc.	The clastic rocks are well-developed in the Maidiping, Qiongzhusi, and Canglangpu formations, while the Longwangmiao Formation is characterized by carbonate rocks. The Qiongzhusi Formation is predominantly composed of argillaceous rocks, whereas the Canglangpu Formation is primarily composed of siltstone and sandstone
Structural Axis Orientation	North-Northeast trending	North-Northeast trending	North-Northwest-trending (near N-S orientation)
Basin Tectono- Sedimentary Framework	One Uplift and Three Depressions	One Uplift and Two Depressions	One trough and two platforms

5.3.3 The extinction period of the Kaijiang-Xuanhan paleo-uplift

In the early stages of the Early Cambrian, the sedimentary-tectonic framework of the Sichuan Basin was no longer entirely controlled by the paleo-uplift; instead, it was jointly influenced by the extensional trough and the paleo-uplift. During the sedimentary period of the lower member of the Qiongzhusi Formation (including the Maidiping Formation) in the Sichuan Basin, the sedimentary center was mainly located in the middle of the Mianyang-Changning extensional trough zone (Figure 8A; Liu et al., 2013). At this stage, the Kaijiang-Xuanhan paleo-uplift may have ceased its activity, and its influence on stratigraphic distribution was primarily due to the paleotopography formed by the earlier paleo-uplift. Therefore, the sedimentary-tectonic framework during the deposition of the lower Qiongzhusi Formation was controlled by the combined influence of the paleotopography formed at the end of the Denying Formation by the Kaijiang-Xuanhan paleo-uplift and the development of the Mianyang- Changning extensional trough (Figure 8A).

Analyzing the thickness map of the upper Qiongzhusi Formation in the Sichuan Basin reveals that the control exerted by the Mianyang- Changning extensional trough became more pronounced. While the paleotopography of the Kaijiang-Xuanhan paleo-uplift still influenced the distribution of stratigraphic thickness, its effect was further diminished (Figures 8A, 10B). The distribution of strata shifted from a northeast to a north-northwest orientation. By this time, the sedimentary-tectonic framework within the basin was primarily governed by the development of the Mianyang- Changning extensional trough, resulting in a structural-sedimentary pattern characterized by one trough (the Mianyang-Changning extensional trough) and two platforms (the flanking platforms on either side of the trough). The Kaijiang-Xuanhan paleo-uplift had essentially disappeared (Table 2).

6 Conclusion

- (1) Through in-depth analysis of data from outcrops around the Sichuan Basin and more than ten newly drilled wells reaching the Dengying Formation within the basin, a detailed tracing and comparison of selected regional framework profiles and 3D seismic profiles have been conducted. This analysis further confirms the existence of the Sinian Kaijiang-Xuanhan paleo-uplift and provides a detailed study of its characteristics. The tectono-sedimentary framework of the entire Sinian system is controlled by this northeast-trending paleo-uplift.
- (2) Both the Kaijiang-Xuanhan area and the Mianyang-Anxian-Changning area exhibit thinning in the Dengying Formation, but the causes differ: in the former, thinning results from early depositional control by the paleo-uplift, with the lower part of stages 1 and 2 missing; in the latter, it is due to later erosional thinning. During the deposition of the Doushantuo and Dengying formations, the Sichuan Basin was likely in a weak compressional state, leading to the formation of the Kaijiang-Xuanhan paleo-uplift, with a northeast-trending structural axis that controlled the deposition and distribution of the Sinian system. By the late deposition of the Dengying Formation and the Early Cambrian, the Sichuan Basin transitioned into a weak extensional state, developing the Mianyang-Changning extensional trough with a north-northwest-trending structural axis, which controlled the deposition of the Lower Cambrian and altered the distribution of the Dengying Formation.
- (3) The Kaijiang-Xuanhan paleo-uplift underwent four stages of evolution: the incubation stage (before the deposition of the Doushantuo Formation), the peak development stage

References

- Bhat, G. M., Craig, J., Hafiz, M., Hakhoo, N., Thurrow, J. W., Thusu, B., et al. (2012). "Geology and hydrocarbon potential of neoproterozoic-cambrian basins in asia: an introduction," in *Geology and hydrocarbon potential of neoproterozoic-cambrian basins in asia*. Editors G. M. Bath, J. Craig, M. Hafiz, N. Hakhoo, J. W. Thurrow, B. Thusu, et al. (Geological Society, London, Special Publications), 366, pp1–17.
- Boger, S., and Miller, J. (2004). Terminal suturing of Gondwana and the onset of the Ross–Delamerian Orogeny: the cause and effect of an Early Cambrian reconfiguration of plate motions. *Earth Planet. Sci. Lett.* 219, 35–48. doi:10.1016/s0012-821x(03)00692-7
- Burchfiel, B. C., Chen, Z., Liu, Y., and Royden, L. H. (1995). Tectonics of the Longmen Shan and adjacent regions, Central China. *Int. Geol. Rev.* 37, 661–735. doi:10.1080/00206819509465424
- Chen, C., and Feng, Q. (2019). Carbonate carbon isotope chemostratigraphy and U–Pb zircon geochronology of the Liuchapo Formation in South China: constraints on the Ediacaran–Cambrian boundary in deep-water sequences. *Palaeoogeogr. Palaeoecol.* 535, 109361. doi:10.1016/j.palaeo.2019.109361
- Chen, D., Zhou, X., Fu, Y., Wang, J., and Yan, D. (2015). New U–Pb zircon ages of the Ediacaran–Cambrian boundary strata in South China. *Terra nova*. 27, 62–68. doi:10.1111/ter.12134
- Chen, H., Lin, C., Zhang, Z., Zhang, D., Zhu, Y., Wu, G., et al. (2021). Depositional characteristics and evolution of miocene deep-water channel systems in block A of lower Congo-Congo fan basin, west Africa. *Petroleum Geol. and Exp.* 2021, 476–486. (in Chinese with English Abstract). doi:10.11781/sydz202103476
- Chen, Z. M., and Chen, Q. Y. (1987). Paleogeography of Yangzi Platform and the characteristics of the phosphorite distribution of early Meishucun stage, early Cambrian. *Chin. J. Geophys.* 22, 246–257. (in Chinese with English Abstract).
- Collins, A. S., and Pisarevsky, S. A. (2005). Amalgamating eastern Gondwana: the evolution of the circum-Indian orogens. *Earth-Science Rev.* 71, 229–270. doi:10.1016/j.earscirev.2005.02.004
- Condon, D. C., Zhu, M. Y., Samuel, B., Wang, W., Yang, A. H., and Jin, Y. G. (2005). U–Pb ages from the neoproterozoic Doushantuo Formation, China. *Science* 308, 95–98. doi:10.1126/science.1107765
- Cozzi, A., Rea, G., and Craig, J. (2012). "From global geology to hydrocarbon exploration: Ediacaran–Early Cambrian petroleum plays of India, Pakistan and Oman," in *Geology and hydrocarbon potential of neoproterozoic cambrian basins in asia*. Editors G. M. Bath, J. Craig, J. W. Thurrow, B. Thusu, and A. Cozzi (Geological Society of London, Special Publication), 131–162.
- Craig, J., Abar, A., Bhat, G., Cadel, G., Hafiz, M., Hakhoo, N., et al. (2013). Hot springs and the geothermal energy potential of Jammu and Kashmir State, N.W. Himalaya, India. *Earth-Science Rev.* 126, 156–177. doi:10.1016/j.earscirev.2013.05.004
- Craig, J., Thurrow, J., Thusu, B., Whitham, A., and Abutarruma, Y. (2009). "Global Neoproterozoic petroleum systems: the emerging potential in North Africa," *Global neoproterozoic petroleum systems: the emerging potential in North Africa*. Editors J. Craig, J. Thurrow, A. Whitham, and Y. Abutarruma (Geological Society, London, Special Publications), 326, pp1–25. doi:10.1144/sp326.1
- Dong, Y. P., Zhang, G. W., Neubauer, F., Liu, X. M., Genser, J., and Hauzenberger, C. (2011). Tectonic evolution of the Qinling orogen, China: review and synthesis. *J. Asian Earth Sci.* 41, 213–237. doi:10.1016/j.jseas.2011.03.002
- Doré, A. G., and Jensen, L. N. (1996). The impact of late Cenozoic uplift and erosion on hydrocarbon exploration: offshore Norway and some other uplifted basins. *Glob. Planet. Change* 12, 415–436. doi:10.1016/0921-8181(95)00031-3
- Ehsan, V., and Abdolrahim, J. (2018). Parameters effective on estimating a nonstationary mixed-phase wavelet using cumulant matching approach. *J. Appl. Geophys.* 148, 83–97. doi:10.1016/j.jappgeo.2017.10.016
- Fernandes, V. M., and Roberts, G. G. (2020). Cretaceous to Recent net continental uplift from paleobiological data: insights into sub-plate support. *GSA Bull.* 133, 1217–1236. doi:10.1130/b35739.1
- Fraser, S. I., Fraser, A. J., Lentini, M. R., and Gawthorpe, R. L. (2007). Return to rifts—the next wave: fresh insights into the petroleum geology of global rift basins. *Pet. Geosci.* 13, 99–104. doi:10.1144/1354-079307-749
- Grotzinger, J., and Al Rawahi, Z. (2014). Depositional facies and platform architecture of microbialite-dominated carbonate reservoirs, Ediacaran–Cambrian Ara Group, Sultanate of Oman. *AAPG Bull.* 98, 1453–1494. doi:10.1306/02271412063
- Gu, Z., Yin, J., Jiang, H., Li, Q., Zhai, X., Huang, P., et al. (2016). Discovery of xuanhan-kaijiang paleouplift and its significance in the Sichuan Basin, SW China. *Petroleum Explor. Dev.* 43, 976–987. doi:10.1016/s1876-3804(16)30115-x
- Han, T., Fan, H., Zhu, X., Wen, H., Zhao, C., and Xiao, F. (2017). Submarine hydrothermal contribution for the extreme element accumulation during the early Cambrian, South China. *Ore Geol. Rev.* 86, 297–308. doi:10.1016/j.oregeorev.2017.02.030
- Huang, J. Z., Cheng, S. J., Song, J. R., Wang, L. S., Gou, X. M., Wang, T. D., et al. (1996). Hydrocarbon system of the Sichuan basin and formation of the medium-to-large gas fields. *Sci. China (Series D)* 26, 504–510. doi:10.1007/BF02878579
- Jacobs, J., and Thomas, R. (2004). Himalayan-type indenter-escape tectonics model for the southern part of the late Neoproterozoic–early Paleozoic East African–Antarctic orogen. *Geology* 32, 721–724. doi:10.1130/g20516.1
- Kang, Y. C. (1988). The formation and development of Paleo-uplift in central Sichuan and its oil/gas prospect. *Exp. Pet. Geol.* 10, 12–23. doi:10.11781/sydz198801012
- Korsch, R. J., Mai, H. Z., Sun, Z. C., and Gortler, J. D. (1991). The Sichuan basin, southwest China: a late Proterozoic (Sinian) petroleum province. *Precambrian Res.* 54, 45–63. doi:10.1016/0301-9268(91)90068-1
- Kumar, V., Ranjan, D., and Verma, K. (2021). "Global climate change: the loop between cause and impact," in *Global climate change* (Elsevier), 187–211.
- Lehmann, B., Frei, R., Xu, L., and Mao, J. (2016). Early cambrian black shale-hosted Mo–Ni and V mineralization on the rifted margin of the Yangtze platform, China: reconnaissance chromium isotope data and a refined metallogenic model. *Econ. Geol.* 111, 89–103. doi:10.2113/econgeo.111.1.89
- Leonov, M. G., Morozov, Y. A., Przhivalovskii, E. S., Rybin, A. K., Bakeev, R. A., Lavrushina, E. V., et al. (2020). Tectonic evolution of the basement–sedimentary cover system and morphostructural differentiation of sedimentary basins. *Geotectonics* 54, 147–172. doi:10.1134/s0016852120020089
- Li, S., Pang, X., Zhang, B., Sun, H., and Sun, A. (2015). Marine oil source of the yingmaili oilfield in the Tarim Basin. *Mar. Petroleum Geol.* 68, 18–39. doi:10.1016/j.marpetgeo.2015.07.016
- Li, S. Z., Santosh, M., Zhao, G. C., Zhang, G. W., and Jin, C. (2012). Intracontinental deformation in a frontier of super-convergence: a perspective on the tectonic milieu of the South China Block. *J. Asian Earth Sci.* 49, 313–329. doi:10.1016/j.jseas.2011.07.026
- Li, W., Liu, J. J., Deng, S. H., Zhang, B. M., and Zhou, H. (2015). The nature and role of Late Sinian–Early Cambrian tectonic movement in Sichuan basin and its adjacent areas. *Acta Pet. Sin.* 36, 546–557. doi:10.7623/syxb201505003
- Li, X. H. (1999). U–Pb zircon ages of granites from the southern margin of the Yangtze block: timing of Neoproterozoic Jinning orogeny in SE China and implications for Rodinia assembly. *Precambrian Res.* 97, 43–57. doi:10.1016/s0301-9268(99)00020-0
- Li, Z., and Zhong, S. (2009). Supercontinent–superplume coupling, true polar wander and plume mobility: plate dominance in whole-mantle tectonics. *Phys. Earth Planet. Interiors* 176, 143–156. doi:10.1016/j.pepi.2009.05.004
- Li, Z. X., and Li, X. H. (2007). Formation of the 1300-km-wide intracontinental orogen and postorogenic magmatic province in Mesozoic South China: a flat-slab subduction model. *Geology* 35, 179–182. doi:10.1130/g23193a.1
- Liu, S., Yang, Y., Deng, B., Zhong, Y., Wen, L., Sun, W., et al. (2021). Tectonic evolution of the Sichuan basin, southwest China. *Earth-Science Rev.* 213, 103470. doi:10.1016/j.earscirev.2020.103470
- Liu, S. G., Deng, B., Li, Z. W., Jansa, L., Liu, S., Wang, G. Z., et al. (2013). Geological evolution of the longmenshan intracontinental composite orogen and the eastern margin of the Tibetan plateau. *J. Earth Sci.* 24, 874–890. doi:10.1007/s12583-013-0391-5
- Liu, S. G., Deng, B., Li, Z. W., and Sun, W. (2012). Architecture of basin-mountain systems and their influences on gas distribution: a case study from the Sichuan basin, South China. *J. Asian Earth Sci.* 47, 204–215. doi:10.1016/j.jseas.2011.10.012
- Liu, S. G., Huang, W. M., Jansa, L. F., Wang, G. Z., Song, G. Y., Zhang, C. J., et al. (2014). Hydrothermal dolomite in the upper sinian (upper proterozoic) Dengying Formation, east Sichuan Basin, China. *Acta Geol. Sin. Engl. Ed.* 88, 1466–1487. doi:10.1111/1755-6724.12312
- Liu, S. G., Ma, Y. S., Sun, W., Cai, X. M., Liu, S., Huang, W. M., et al. (2008). Studying the differences of Sinian Natural gas pools between Weiyuan gas field and Ziyang gas-brone area, Sichuan basin. *Acta Geol. Sin.* 82, 328–227. (in Chinese with English Abstract).
- Liu, S. G., Qin, C., Jansa, L., Sun, W., Wang, G. Z., Xu, G. S., et al. (2011). Transformation of oil pools into gas pools as results of multiple tectonic events in Upper Sinian (Upper Neoproterozoic), deep part of Sichuan Basin, China. *Energy Explor. and Exploitation* 29, 679–698. doi:10.1260/0144-5987.29.6.679
- Lottaroli, F., Craig, J., and Thusu, B. (2009). "Neoproterozoic-early cambrian (infracambrian) hydrocarbon prospectivity of North Africa: a synthesis," *Global neoproterozoic petroleum systems: the emerging potential in North Africa*. Editors J. Craig, J. Thurrow, A. Whitham, and Y. Abutarruma (Geological Society, London, Special Publications), 326, 137–156. doi:10.1144/sp326.7
- Ma, Y. S., Guo, X. S., Guo, T. L., Huang, R., Cai, X. Y., and Li, G. X. (2007). The Puguang gas field: new giant discovery in the mature Sichuan basin, southwest China. *AAPG Bull.* 91, 627–643. doi:10.1306/110306060602
- Maruyama, S., Santosh, M., and Zhao, D. (2007). Superplume, supercontinent, and post-perovskite: mantle dynamics and anti-plate tectonics on the Core–Mantle Boundary. *Gondwana Res.* 11, 7–37. doi:10.1016/j.gr.2006.06.003
- Meert, J., and Torsvik, T. (2003). The making and unmaking of a supercontinent: Rodinia revisited. *Tectonophysics* 375, 261–288. doi:10.1016/s0040-1951(03)00342-1

- Meng, F., Ni, P., Schiffbauer, J., Yuan, X., Zhou, C., Wang, Y., et al. (2011). Ediacaran seawater temperature: evidence from inclusions of Sinian halite. *Precambrian Res.* 184, 63–69. doi:10.1016/j.precamres.2010.10.004
- Narbonne, G. M., and Aitken, J. D. (1995). Neoproterozoic of the mackenzie mountains, northwestern Canada. *Precambrian Res.* 73, 101–121. doi:10.1016/0301-9268(94)00073-z
- Okada, Y., Sawaki, Y., Komiya, T., Hirata, T., Takahata, N., Sano, Y., et al. (2014). New chronological constraints for cryogenian to cambrian rocks in the three gorges, weng'an and chengjiang areas, south China. *Gondwana Res.* 25, 1027–1044. doi:10.1016/j.jgr.2013.05.001
- Peters, J. M., Filbrandt, J. B., Grotzinger, J. P., Newall, M. J., Shuster, M. W., and Al-Siyabi, H. A. (2003). Surface-piercing salt domes of interior North Oman, and their significance for the Ara carbonate stringer hydrocarbon play. *GeoArabia* 8, 231–270. doi:10.2113/geoarabia0802231
- Rino, S., Kon, Y., Sato, W., Maruyama, S., Santosh, M., and Zhao, D. (2008). The Grenvillian and Pan-African orogens: world's largest orogenies through geologic time, and their implications on the origin of superplume. *Gondwana Res.* 14, 51–72. doi:10.1016/j.jgr.2008.01.001
- Santosh, M., Maruyama, S., and Yamamoto, S. (2009). The making and breaking of supercontinents: some speculations based on superplumes, super downwelling and the role of tectosphere. *Gondwana Res.* 15, 324–341. doi:10.1016/j.jgr.2008.11.004
- Sato, H., Tahata, M., Sawaki, Y., Maruyama, S., Yoshida, N., Shu, D., et al. (2016). A high-resolution chemostratigraphy of post-Marinoan Cap Carbonate using drill core samples in the Three Gorges area, South China. *Geosci. Front.* 7, 663–671. doi:10.1016/j.gsf.2015.07.008
- Saylor, B. Z., Grotzinger, J. P., and Germs, G. J. B. (1995). Sequence stratigraphy and sedimentology of the neoproterozoic kuibis and schwarstrand subgroups (nama group), southwestern Namibia. *Precambrian Res.* 73, 153–171. doi:10.1016/0301-9268(94)00076-4
- Shang, Y. X., Gao, Z. Q., Fan, T. L., Wei, D., Wang, Z. Y., and Karubandika, G. M. (2020). The Ediacaran–Cambrian boundary in the Tarim Basin, NW China: geological data anomalies and reservoir implication. *Mar. Petroleum Geol.* 111, 557–575. doi:10.1016/j.marpetgeo.2019.08.032
- Slack, P. B. (1981). Paleotectonics and hydrocarbon accumulation, powder river basin, Wyoming. *AAPG Bull.* 65, 730–743. doi:10.1306/2f9199bd-16ce-11d7-8645000102c1865d
- Smith, A. G. (2012). “A review of the Ediacaran to Early Cambrian (“Infra-Cambrian”) evaporites and associated sediments of the Middle East,” in *Geology and hydrocarbon potential of neoproterozoic-cambrian basins in asia*. Editors G. M. Bath, J. Craig, M. Hafiz, N. Hakhoo, J. W. Thurow, B. Thusu, et al. (Geological Society, London, Special Publications), 366, 229–250.
- Steiner, M., Li, G., Qian, Y., Zhu, M., and Erdtmann, B. D. (2007). Neoproterozoic to Early Cambrian small shelly fossil assemblages and a revised biostratigraphic correlation of the Yangtze Platform (China). *Palaeogeogr. Palaeoclimatol. Palaeoecol.* 254, 67–99. doi:10.1016/j.palaeo.2007.03.046
- Tang, J., Hu, W., Li, W., and Zhang, G. (2013). Prediction of weathering paleokarst reservoirs by combining paleokarst landform with unconformity: a case study of Sinian Dengying Formation in Leshan-Longnüsi paleo-uplift, Sichuan Basin. *Petroleum Explor. Dev.* 40, 722–730. doi:10.1016/s1876-3804(13)60097-x
- Valdiya, K. S. (1995). Proterozoic sedimentation and Pan-African geodynamic development in the Himalaya. *Precambrian Res.* 74, 35–55. doi:10.1016/0301-9268(95)00004-o
- Wang, C., Tang, H., Zheng, Y., Dong, L., Li, J., and Qu, X. (2019). Early Paleozoic magmatism and metallogeny related to Proto-Tethys subduction: insights from volcanic rocks in the northeastern Altyn Mountains, NW China. *Gondwana Res.* 75, 134–153. doi:10.1016/j.jgr.2019.04.009
- Wang, G. Z., Liu, S. G., Chen, C. H., Wang, D., and Sun, W. (2013). The genetic relationship between MVT Pb-Zn deposits and paleo-oil/gas reservoirs at Heba, southeastern Sichuan basin. *Earth Sci. Front.* 20, 107–116. (in Chinese with English Abstract).
- Wang, J., Wang, X., Cao, Y., Hao, F., Pang, Y., Yun, L., et al. (2024). Characteristics and origin of the ultradeep Ordovician fault-karst reservoirs: an example from the Shunbei-Yuejin area, Tarim Basin. *AAPG Bull.* 108, 1231–1260. doi:10.1306/10052321152
- Wang, J. G., Chen, D. Z., Wang, D., Yan, D., Zhou, X. Q., and Wang, Q. C. (2012). Petrology and geochemistry of chert on the marginal zone of Yangtze platform, western Hunan, South China, during the Ediacaran-Cambrian transition. *Sedimentology* 59, 809–829. doi:10.1111/j.1365-3091.2011.01280.x
- Wang, J. Q. (1996). Relationship between tectonic evolution and hydrocarbon in the foreland of the Longmen mountains. *J. Southeast Asian Earth Sci.* 13, 327–336. doi:10.1016/0743-9547(96)00039-6
- Yu, J. H., O'Reilly, S. Y., Wang, L., Griffin, W. L., Zhang, M., Wang, R., et al. (2008). Where was South China in the Rodinia supercontinent? Evidence from U-Pb geochronology and Hf isotopes of detrital zircons. *Precambrian Res.* 164, 1–15. doi:10.1016/j.precamres.2008.03.002
- Zhao, G., and Cawood, P. A. (2012). Precambrian geology of China. *Precambrian Res.* 222–223, 13–54. doi:10.1016/j.precamres.2012.09.017
- Zhong, C., and Huang, J. (1997). Drilling and gas recovery technology in ancient China. Zigong Salt Industry Museum. *Zigong, Sichuan, PRC*.
- Zhong, Y., Li, Y. L., Zhang, X. B., Liu, S. G., Wu, F. R., Liu, D. J., et al. (2014). Evolution characteristics of central Sichuan palaeouplift and its relationship to Early Cambrian Mianyang-Changning intracratonic sag. *J. Chengdu Univ. Technol. Sci. and Technol. Ed.* 41, 703–713. (in Chinese with English Abstract).
- Zhou, C. N., Du, J. H., Xe, C. C., Wang, Z. C., Zhang, B. M., Wei, G. Q., et al. (2014). Formation, distribution, resource potential and discovery of the Sinian-Cambrian giant gas field, Sichuan Basin, SW China. *Petroleum Explor. Dev.* 41, 278–293. doi:10.1016/S1876-3804(14)60036-7
- Zhou, M. F., Yan, D. P., Vasconcelos, P. M., Li, J. W., and Hu, R. Z. (2008). Structural and geochronological constraints on the tectono-thermal evolution of the Danba domal terrane, eastern margin of the Tibetan Plateau. *J. Southeast Asian Earth Sci.* 33, 414–427. doi:10.1016/j.jseae.2008.03.003
- Zhu, G. Y., Wang, T. S., Xie, Z. Y., Xie, B. H., and Liu, K. Y. (2015). Giant gas discovery in the Precambrian deeply buried reservoirs in the Sichuan basin, China: implications for gas exploration in old cratonic basins. *Precambrian Res.* 262, 45–66. doi:10.1016/j.precamres.2015.02.023